RSC Advances

PAPER

View Article Online
View Journal | View Issue

Cite this: *RSC Adv.*, 2019, **9**, 1526

Synthesis and thermally induced structural transformation of phthalimide and nitrile-functionalized benzoxazine: toward smart *ortho*-benzoxazine chemistry for low flammability thermosets†

Kan Zhang, *[a] Yuqi Liu,[a] Lu Han,[b] Jinyun Wang[a] and Hatsuo Ishida*[b]

A novel *ortho*-phthalimide-functionalized benzoxazine monomer containing an *ortho*-nitrile group has been synthesized in order to further systematically evaluate the thermally induced structural transformation from benzoxazine resin to cross-linked polybenzoxazole. The chemical structure of the synthesized monomer has been confirmed by ^{1}H and ^{13}C nuclear magnetic resonance (NMR) spectroscopy and Fourier transform infrared (FT-IR) spectroscopy. Also supporting the detailed structure is ^{1}H–^{13}C heteronuclear multiple quantum coherence (HMQC), which identifies the local proton-carbon proximities. The polymerization behaviors, including the ring-opening polymerization of the oxazine rings and the cyclotrimerization of the nitrile functionalities, are studied by differential scanning calorimetry (DSC) and *in situ* FT-IR. In addition, the subsequent benzoxazole formation after polymerization has also been analyzed using thermogravimetric analysis (TGA) and magic-angle spinning (MAS) solid-state ^{13}C NMR. The resulting cross-linked polybenzoxazole derived from the benzoxazine monomer exhibits exceptionally high thermal stability and low flammability, with an extremely high T_{d5} temperature (550 °C), a high char yield value (70%) and an extraordinarily low total heat release (THR of 7.6 kJ g^{-1}).

Received 5th December 2018
Accepted 26th December 2018

DOI: 10.1039/c8ra10009h

rsc.li/rsc-advances

Introduction

There is growing interest in aromatic polymers with excellent mechanical and thermal properties to meet the crucial requirements of aerospace and electronic technology. Among the many polymeric materials, aromatic polybenzoxazoles (PBOs) are a class of heterocyclic polymers possessing superb thermal stability, extremely high tensile strength, and excellent chemical resistance.[1] In general, there are two traditional methods for the synthesis of aromatic PBOs. The first method is one-step synthesis, in which a direct polycondensation takes place between bis(*o*-aminophenol)s and aromatic diacids using poly(phosphoric acid) (PPA),[2] phosphorus pentoxide/methanesulfonic acid (PPMA),[3] or trimethylsilyl polyphosphate (PPSE)/*o*-dichlorobenzene[4] as the reaction medium. This approach is normally applied for producing PBO fibers. However, the residual acid in PBO fibers easily causes hydrolytic degradation of the benzoxazole moiety when exposed to moisture at moderate to elevated temperatures.[5] The second method for the synthesis PBO consists of two steps; first is a condensation reaction of an aromatic diacid chloride with a bis(*o*-aminophenol) in an organic solvent at room temperature to form a poly(*o*-hydroxyamide), followed by a sequential thermal intramolecular cyclodehydration reaction in the bulk state or in solution with the loss of water to yield the final aromatic polybenzoxazole.[6–9] In addition, some researchers also reported the possible thermally induced structural transformation of *o*-hydroxypolyimides into polybenzoxazoles with the loss of carbon dioxide at temperatures of around 400 °C.[10–14]

Although the highly rigid molecular structure of PBOs brings outstanding performance, it also causes difficulties in synthesis and fabrication. For example, the wholly aromatic PBOs are soluble only in harsh acids. Besides, no glass transition temperature (T_g) can be observed before their decomposition temperature, which impedes the melt processing of PBOs. Furthermore, bis(*o*-aminophenol)s used as the main starting materials for most synthesis approaches of PBOs are expensive.[15] All of the above shortcomings result in the limited application of this class of high-performance polymers.

Polybenzoxazines,[16–18] as a novel type of thermoset, offer outstanding advantages such as high thermal stability,[19] high

[a]*School of Materials Science and Engineering, Jiangsu University, Zhenjiang 212013, China. E-mail: zhangkan@ujs.edu.cn*

[b]*Department of Macromolecular Science and Engineering, Case Western Reserve University, Cleveland, OH, 44106, USA. E-mail: hxi3@cwru.edu*

† Electronic supplementary information (ESI) available. See DOI: 10.1039/c8ra10009h

char yield,[20] high T_g,[21] near-zero volumetric change during polymerization,[22] good mechanical[23] and dielectric properties,[24] low water absorption[25] and low flammability.[26] Various forms of hydrogen-bonding within the final network structure are observed in polybenzoxazines, contributing greatly to their unique properties.[27] Besides, the potential for rich molecular design flexibility is one of the most attractive properties of this class of polymers.

A series of benzoxazines with imide functionality have been developed by taking advantage of the molecular design flexibility of benzoxazine chemistry.[19,28–30] One of the particularly interesting features of these imide-functionalized benzoxazines is their ability to be the precursor for further structural transformation to polybenzoxazoles, which exhibit very high thermal stability with a T_{d5} temperature as high as 505 °C in a nitrogen atmosphere.[19] Additionally, the *ortho*-imide-functionalized benzoxazines show great advantages in the synthesis of polybenzoxazoles, since no harsh acids are required. The research of *ortho*-imide benzoxazines suggests the possibility to form high performance thermosets from simple low molecular weight compounds.

Previously, benzoxazine resins containing nitrile moieties have been widely studied since incorporation of the nitrile functionality results in an increased char yield, thereby leading to low flammability.[31,32] Interestingly, it was reported that the polybenzoxazine derived from monofunctional benzoxazine containing a nitrile functionality at the *ortho* position with respect to the nitrogen group in the oxazine ring showed the best thermal stability when compared with polybenzoxazines polymerized form *para*- and *meta*-nitrile functional benzoxazine analogues.[31]

Inspired by the smart *ortho* approach for developing high performance thermosets in benzoxazine chemistry, a novel fully *ortho*-functionalized benzoxazine monomer containing phthalimide and nitrile functionalities at *ortho* positions with respect to the oxygen and nitrogen in the oxazine ring, respectively, has been synthesized in this study. In continuation of our previous studies on the *ortho*-imide-functionalized benzoxazines, the aim of this study is to further develop a very high thermal stability thermoset with ultra-low flammability by incorporating an *ortho*-nitrile group. Furthermore, thermally induced structural transformation, including ring-opening polymerization, cyclotrimerization and benzoxazole formation, is also systematically investigated.

Experimental

Materials

o-Aminophenol, anthranilonitrile, phthalic anhydride, and paraformaldehyde (99%) were used as received from Sigma-Aldrich. Acetic acid, methanol, *N*,*N*-dimethylformamide (DMF) and xylenes were kindly supplied by East Instrument Chemical Glass Co., Ltd., China and used as received. The starting phenol, 2-(2-hydroxyphenyl)-isoindoline-1,3-dione (*o*-PP), and the benzoxazine monomer, 2-(3-phenyl-3,4-dihydro-2*H*-benzo[*e*][1,3]oxazin-8-yl)-isoindoline-1,3-dione (*o*PP-a), were synthesized according to the literature with slight modification (see ESI, Fig. S1–S4†).[19]

Synthesis of 2-(8-(1,3-dioxoisoindolin-2-yl)-2*H*-benzo[*e*][1,3]oxazin-3(4*H*)-yl)benzonitrile (*o*PP-an)

In a 150 mL round flask were mixed 50 mL of xylenes, anthranilonitrile (1.77 g, 0.015 mol), *o*-PP (3.59 g, 0.015 mol), and paraformaldehyde (0.96 g, 0.032 mol). The mixture was stirred at 120 °C for 8 h. Afterwards, the reaction solution was cooled to room temperature and precipitated into 100 mL of methanol. Removal of the solvent by filtering afforded a white powder (yield *ca.* 91%, mp 251 °C). ^{1}H NMR (DMSO), ppm: $\delta = 4.80$ (s, Ar–CH_2–N, oxazine), 5.40 (s, O–CH_2–N, oxazine), 6.91–7.99 (11H, Ar). IR spectra (KBr), cm^{-1}: 2221 (C≡N stretching of nitrile group) 1774, 1720 (imide I), 1492 (stretching of trisubstituted benzene ring), 1385 (imide II), 1229 (C–O–C asymmetric stretching), 1168 (C–N–C asymmetric stretching), 938 (oxazine ring related mode).

Preparation of polybenzoxazine (poly(*o*PP-an)) and cross-linked polybenzoxazole (PBO-*o*PP-an)

A solution containing 30% solid of the monomer in DMF was prepared in a flask at room temperature. Then, the solution was cast over a dichlorodimethylsilane-pretreated steel plate. The film was dried in an air circulating oven at 120 °C for 2 days to remove the solvent completely. The film as fixed to the plate was polymerized stepwise at 160, 180, 200, 220, 240 and 260 °C for 1 h each to obtain poly(*o*PP-an). Heat treatment of poly(*o*PP-an) was further carried out in a tube furnace under a steady flow of N_2 at 400 °C for 1 h to obtain PBO-*o*PP-an.

Characterization

A Bruker AVANCE II nuclear magnetic resonance (NMR) spectrometer was used to obtain ^{1}H and ^{13}C NMR spectra at a proton frequency of 400 MHz, in DMSO-d_6 using tetramethyl silane as an internal standard. The average number of transients for ^{1}H and ^{13}C NMR measurement was 64 and 1024, respectively. ^{1}H–^{13}C heteronuclear multiple quantum coherence (HMQC) was also carried out. Cross-polarization magic-angle spinning (CP-MAS) solid-state ^{13}C NMR spectra were collected using a Bruker Avance III 400 MHz instrument, using adamantane as a reference. Powder samples were packed into a 4 mm zirconia rotor with a spinning rate of 10 000 Hz, and the number of transients was 6000 scans. FTIR measurements were recorded on a Nicolet Nexus 670 Fourier transform infrared (FTIR) spectrophotometer in the range of 4000–400 cm^{-1}. A NETZSCH DSC model 204F1 was used with a temperature ramp rate of 10 °C min^{-1} under a nitrogen atmosphere, and the flow rate of nitrogen was 60 mL min^{-1} for the differential scanning calorimetric (DSC) study. In the analyses to determine the activation energy of polymerization, the samples (2.0 ± 0.5 mg) were scanned at different heating rates of 2, 5, 10, 15, 20 °C min^{-1}. Thermogravimetric analyses (TGA) were conducted on a NETZSCH STA449C Thermogravimetric Analyzer. Nitrogen at a flow rate of 40 mL min^{-1} was purged. For the isothermal TGA, the temperature program was room temperature to 800 °C at the

heating rate of 10 °C min^{-1} under nitrogen at a flow rate of 40 mL min^{-1} and holding the temperature at 400 °C for 1 h. The specific heat release rate (HRR, W g^{-1}), heat release capacity (HRC, J (g K)$^{-1}$) and total heat release (THR, kJ g^{-1}) were measured on a microscale combustion calorimeter (MCC) from PHINIX Co., Ltd. MCC was carried out from 100 to 900 °C at a heating rate of 1 °C s^{-1} in an 80 cm^3 min^{-1} stream of nitrogen. The anaerobic thermal degradation products in the nitrogen gas stream were mixed with a 20 cm^3 min^{-1} stream of oxygen prior to entering the combustion furnace (900 °C). Heat release is quantified by standard oxygen consumption,[33] and HRR is obtained by dividing dQ/dt at each time interval by the initial sample mass. Moreover, HRC can be obtained by dividing the maximum value of HRR by the heating rate.

Results and discussion

Synthesis of the *ortho*-phthalimide-functionalized benzoxazine monomer containing a nitrile group

The successful synthesis of a fully *ortho*-functionalized benzoxazine monomer containing a phthalimide and nitrile group has been achieved using anthranilonitrile, formaldehyde, and *ortho*-phthalimide-functionalized phenol, as shown in Scheme 1. The obtained benzoxazine in this study exhibited advantages in synthesis from the viewpoints of short reaction time (8 h), high yield (91%) and ease of purification, which supports the superior properties of *ortho*-benzoxazine resins.

The structure of the monomer, *o*PP-an, has been confirmed using ^{1}H NMR spectra, as depicted in Fig. 1. The typical resonances attributed to the benzoxazine structure, Ar–CH_2–N– and –O–CH_2–N– for *o*PP-an are observed at 4.80 and 5.40 ppm, respectively. In addition, the ^{13}C NMR spectrum shown in Fig. 2 is applied to confirm the characteristic signal of the oxazine ring and nitrile group. The characteristic carbon resonances of the oxazine ring are assigned at 51.78 and 80.53 ppm for Ar–*C*H_2–N– and –O–*C*H_2–N–, respectively. Moreover, the ^{13}C NMR spectrum of *o*PP-an shows a characteristic resonance at 106.48 ppm corresponding to the nitrile carbon of –*C*≡N. The above assignments for the oxazine protons and carbons, and nitrile carbon in the structure of *o*PP-an are supported by the ^{1}H–^{13}C HMQC NMR analysis (Fig. S5†).

A number of infrared absorption bands are highlighted as shown in Fig. 3, which are used to further verify the existence of the oxazine ring and nitrile functionality in the molecular

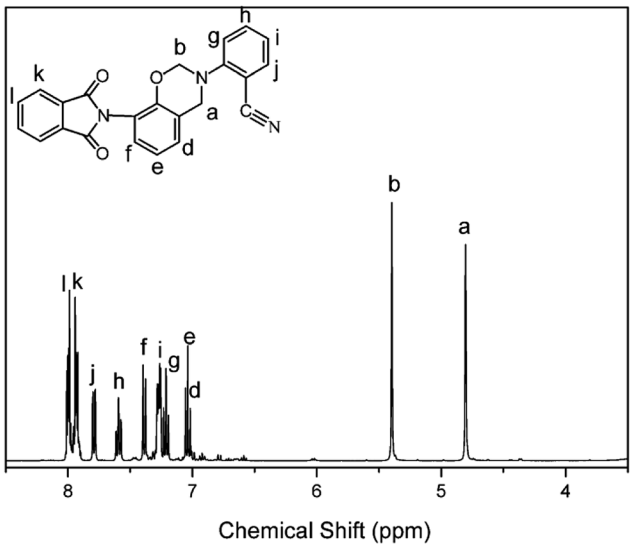

Fig. 1 ^{1}H NMR spectrum of *o*PP-an.

structure. For example, the characteristic band at 2221 cm^{-1} is due to the C≡N stretching of the nitrile group. The characteristic doublet peaks at 1784 cm^{-1} and 1720 cm^{-1} are the typical bands for imide, and are attributed to the imide C–C(=O)–C antisymmetric and symmetric stretching, respectively.[34] In addition to these bands, the presence of imide is seen by the other characteristic band at 1385 cm^{-1}, which is due to the axial stretching of C–N bonds.[35,36] The band characteristic of antisymmetric trisubstituted benzene that appears at 1492 cm^{-1} confirms the incorporation of an imide group into the benzoxazine monomer. Besides, the presence of the benzoxazine ring aromatic ether in the monomer is indicated by the band centered at 1229 cm^{-1} due to the C–O–C antisymmetric stretching modes.[37] Furthermore, the characteristic oxazine-related mode is located at 938 cm^{-1}.[38] The FT-IR spectrum further supports the structure of the *o*PP-an obtained.

Polymerization behavior of the benzoxazine monomer

The polymerization behavior of *o*PP-an was studied by DSC, and the corresponding thermogram is depicted in Fig. 4. Ordinarily, the characteristic thermogram for a benzoxazine monomer consists of an endothermic peak as well as an exothermic peak due to the melting and ring-opening polymerization behaviors.

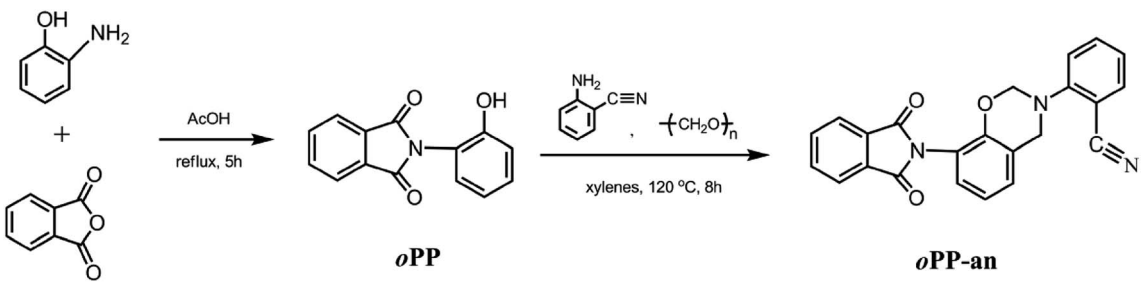

Scheme 1 Synthesis of the *ortho*-phthalimide functional benzoxazine monomer containing a nitrile group.

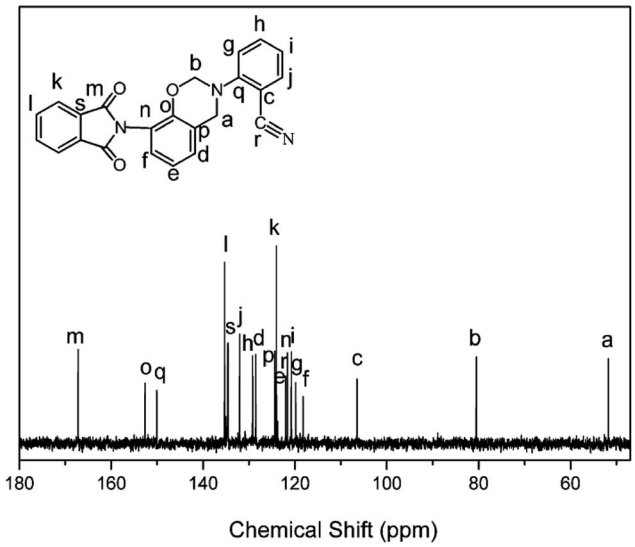

Fig. 2 ^{13}C NMR spectrum of *o*PP-an.

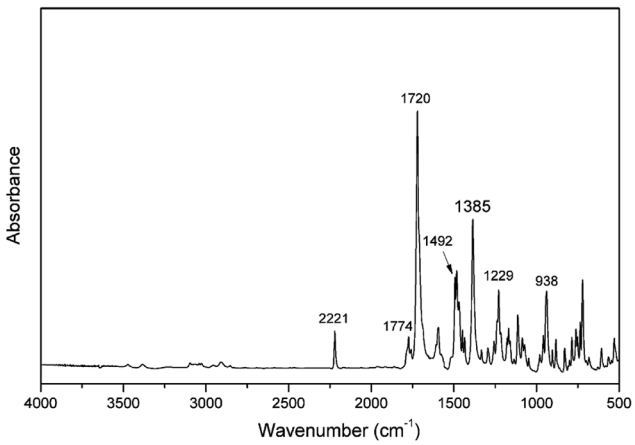

Fig. 3 FTIR spectrum of the benzoxazine monomer.

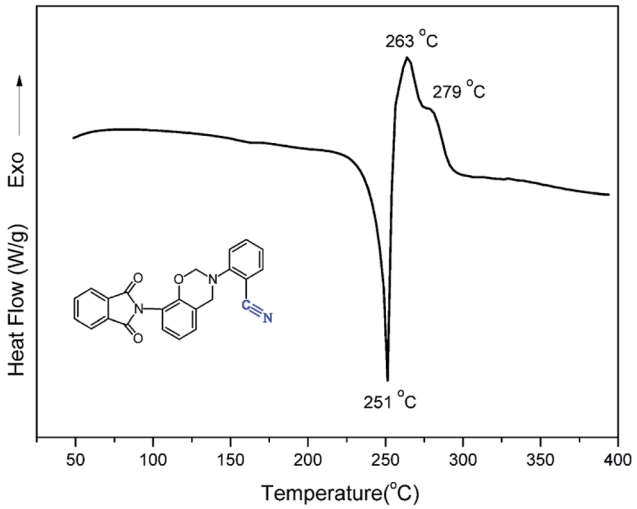

Fig. 4 DSC polymerization behavior of a mono-functionalized benzoxazine monomer.

For example, the *ortho*-phthalimide-functionalized benzoxazine without a nitrile functionality, *o*PP-a, was reported to show an endothermic peak at 209 °C and an exothermic peak at 234 °C.[39] Herein, after incorporating the nitrile functionality, the thermogram of *o*PP-an shows a very sharp endothermic peak at a temperature as high as 251 °C. This sharp melting peak further indicates the excellent purity of *o*PP-an. Subsequently, as can be seen in the figure, there are two exothermic peaks with maxima at 263 and 279 °C, respectively. The high melting temperature causes a partial overlap between the melting and polymerization behaviors. To the best of our knowledge, this unique DSC thermogram with such a high temperature and very sharp endothermic peak was observed for the first time for a benzoxazine monomer. The rigidity, originating from the combination of the imide structure with an aromatic structure and nitrile group, led to *o*PP-an having a higher melting temperature compared with other traditional benzoxazine monomers. In general, a trade-off exists between the synthesis and properties of polymers. Polymers with highly rigid structures normally possess superior properties, but suffer difficulties during the synthesis and processing procedures. For example, a highly polar solvent or high temperature is always required for the preparation of polyimides or polybenzoxazoles. However, the synthesis process for *o*PP-an with high rigidity only requires a low polarity solvent (xylenes) and short reaction time (8 h), showing the advantages of the synthesis of high performance polymers *via ortho*-phthalimide-functionalized benzoxazines. Additionally, the multiple exotherms of *o*PP-an can be considered as two different cross-linking processes, namely, the ring-opening polymerization of the oxazine as well as the cyclotrimerization of the nitrile group, which occur separately. However, the enthalpy for each polymerization of *o*PP-an cannot be detected since the multiple thermal behaviors occur in a narrow temperature range.

In order to qualitatively study the structural evolution during polymerization, *in situ* FT-IR analyses were carried out and the spectra for *o*PP-an are displayed in Fig. 5. As shown in Fig. 5, no obvious changes can be observed for all of the absorption bands of *o*PP-an before 200 °C. This result is in agreement with the DSC profile, suggesting that no types of polymerization take place before the melting behavior. The characteristic absorption bands at 1229 cm^{-1} (C–O–C asymmetric stretching modes) and 938 cm^{-1} (the oxazine ring related mode) gradually disappear from 200 to 220 °C. Meanwhile, a broad band of –OH between 3500 and 3300 cm^{-1} gradually appears, indicating the completion of the ring-opening polymerization of the oxazine rings. Additionally, as shown in Fig. 6, an intensity decrease of the band at 2221 cm^{-1} (C≡N stretching) is observed, and new bands appear gradually at 1621 cm^{-1} (C=N stretching) and 1381 cm^{-1} (triazine related mode) from 220 °C, suggesting the cyclotrimerization of the nitrile functionality. Furthermore, the characteristic absorption band for nitrile at around 2221 cm^{-1} mostly disappeared after the thermal treatment at 260 °C for 1 h. Both Fig. 5 and 6 provide reliable information on the order of these two events taking place. From these results, it is

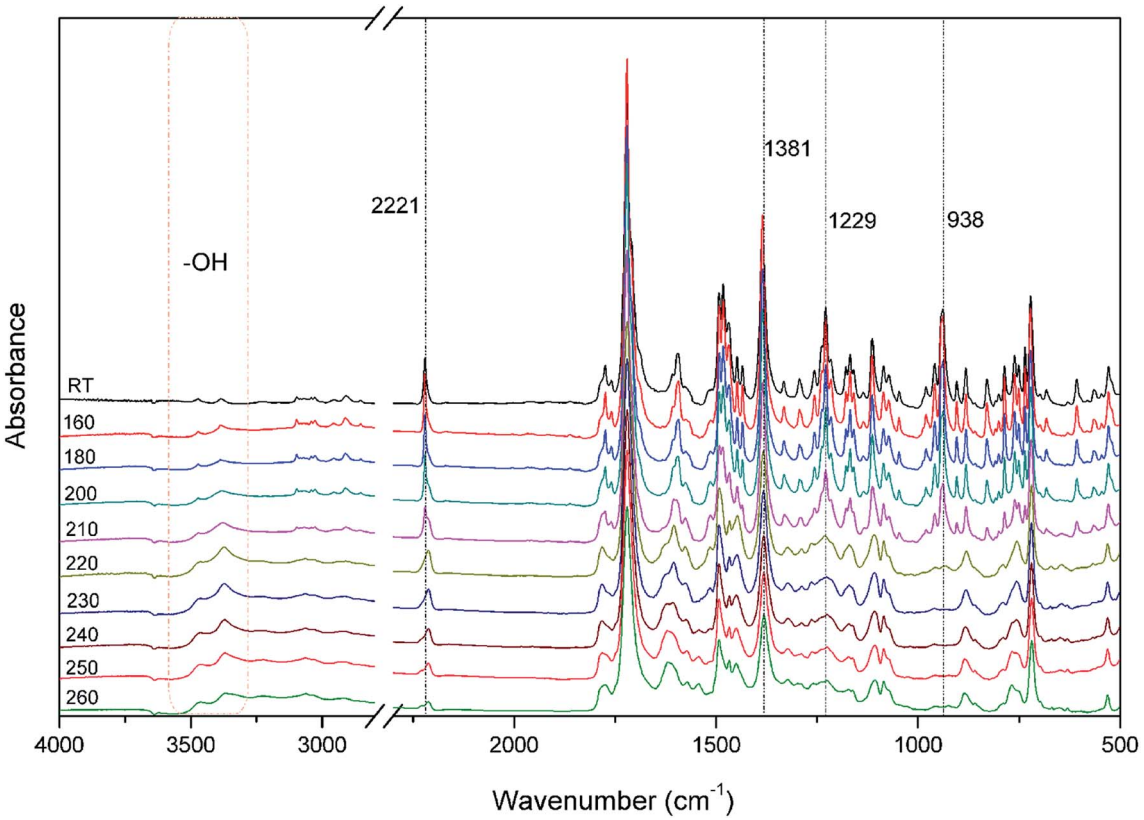

Fig. 5 FT-IR spectra of *o*PP-an after various thermal treatments at each designed temperature stage for 1 h.

determined that the ring-opening polymerization of the oxazine ring takes place first at 220 °C, while the nitrile functionality subsequently cyclotrimerizes at a relatively higher temperature. Therefore, the orders of the two exothermic peaks from the above DSC results can be clearly established, namely benzoxazine ring-opening polymerization first, and then the cyclotrimerization of the nitrile group.

Fig. 7 shows the DSC profiles of *o*PP-an at heating rates of 2, 5, 10, 15 and 20 °C min^{-1}, respectively. The thermograms of *o*PP-an show that the endothermic peaks and exothermic peaks shift to higher temperatures with an increase of heating rate. The activation energy of the polymerization process was determined using the well-known Kissinger and Ozawa methods.[40,41] According to the Kissinger method, the activation energy can be calculated using eqn (1) as follows:

$$\ln\left(\frac{\beta}{T_p^2}\right) = \ln\left(\frac{AR}{E_a}\right) - \frac{E_a}{RT_p} \quad (1)$$

where β is the heating rate, A is the frequency factor, T_p is the temperature of the exothermic peak, E_a is the activation energy, and R is the gas constant. If the plot of $\ln(\beta/T_p^2)$ against $1/T_p$ is linear, E_a can be obtained from the slope of the corresponding straight line.

Another theoretical treatment, namely, the Ozawa method, can also be applied to the thermal data using eqn (2) as follows:

$$\ln \beta = -1.052\frac{E_a}{RT_p} + C \quad (2)$$

where C is a constant.

Fig. 8 and 9 show the plot of $\ln(\beta/T_p^2)$ or $\ln(\beta)$ against $1/T_p$ for *o*PP-an according to the Kissinger and Ozawa methods. The activation energies calculated from the slopes of the Kissinger and Ozawa plots of the first exotherm are 146.4 and 147.2 kJ mol^{-1}. Besides, those from the second exotherm are estimated to be 111.5 and 114.6 kJ mol^{-1}, respectively, as shown in Table 1. The activation energies obtained for the first exotherm are much higher than that of *o*PP-a, which was estimated to be 86.0 kJ mol^{-1} (Kissinger) and 89.5 kJ mol^{-1} (Ozawa) (Fig. S6, S7 and Table S1†). The only difference between *o*PP-a and *o*PP-an is the existence of a nitrile functionality at the *ortho* position with respect to the nitrogen in the oxazine ring in *o*PP-an, by considering their molecular structures. Thus, the high activation energy for the first exotherm of the ring-opening polymerization of the oxazine ring is proposed to be caused by incorporating a nitrile functionality into the benzoxazine structure, leading to higher rigidity of the molecule itself. However, the estimated activation energy for both exotherms is lower than that of some other reported amide-functionalized or imide-functionalized benzoxazines, which are regarded as precursors for high-performance materials.[39] Therefore, *o*PP-an can be easily activated to polymerize in terms of benzoxazine resins for high-performance applications. Additionally, the apparent activation energies for both exotherms of *o*PP-an reported above are an average value of those processes, and thus should be considered only as a guide since the maxima of the two exotherms heavily overlap.

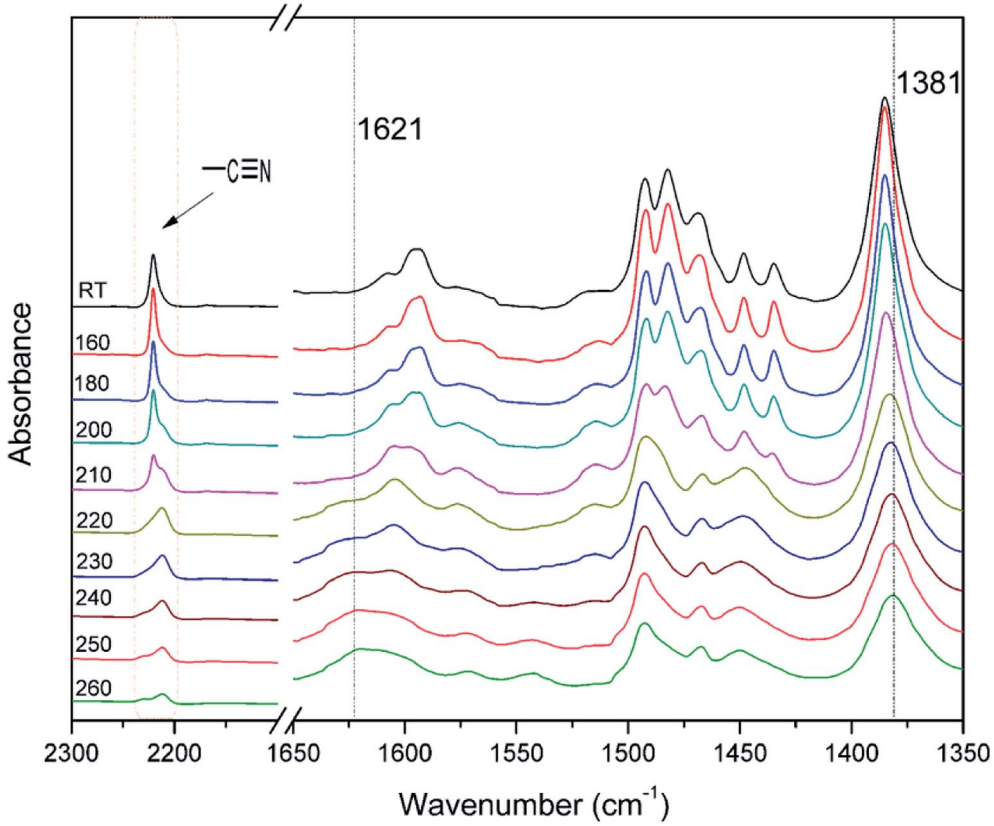

Fig. 6 Expansion of the FT-IR spectra for *o*PP-an after various thermal treatments in the range of 2300 to 1350 cm^{-1}.

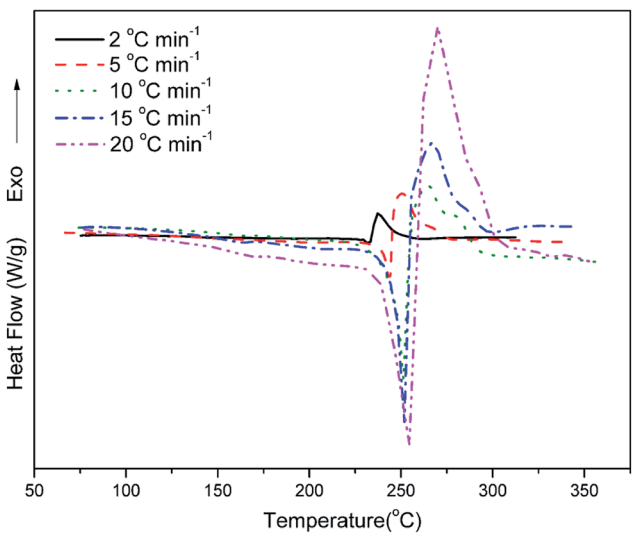

Fig. 7 DSC curves of *o*PP-an at different heating rates.

Thermally induced structural transformation

It has been established that the *ortho*-imide polybenzoxazines undergo thermally induced structural transformation by further thermal treatment into another class of polymer, specifically, cross-linked polybenzoxazoles. However, benzoxazole formation from *ortho*-imide benzoxazines was only supported by evidence from FT-IR analyses.[19] In order to qualitatively study the structural evolution of *o*PP-an during heating, TGA and solid-state ^{13}C NMR analyses were carried out.

TGA curves of a representative sample of poly(*o*PP-an) are shown in Fig. 10. Poly(*o*PP-an) shows a bimodal degradation profile in which the first maximum weight-loss rate is at 381 °C, which corresponds to the typical benzoxazole formation temperature. Besides, the second maximum weight loss rate is located at 640 °C, which is in agreement with the maximum degradation weight-loss rate of benzoxazole groups. Marked on

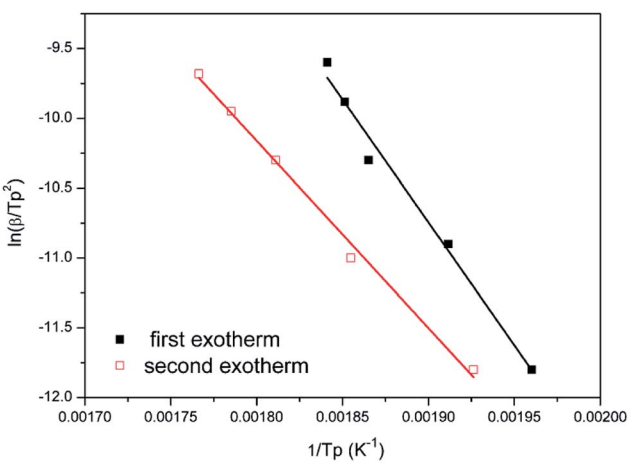

Fig. 8 Representations of the Kissinger method for the calculation of the activation energy for *o*PP-an.

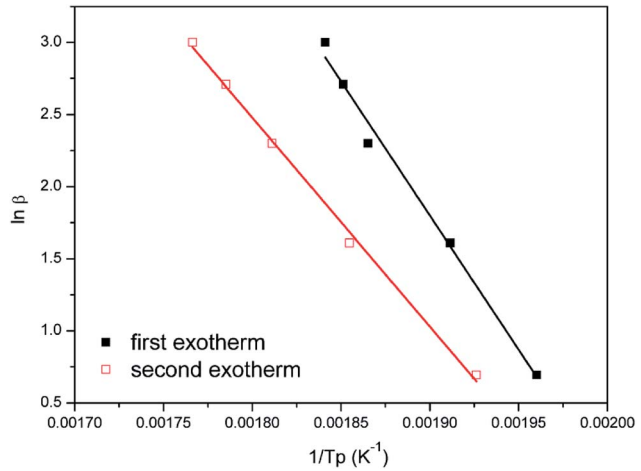

Fig. 9 Representations of the Ozawa method for the calculation of the activation energy for *o*PP-an.

Table 1 The activation energy of *o*PP-an obtained by the Kissinger and Ozawa methods

	Kissinger	Ozawa
	E_a (kJ mol^{-1})	E_a (kJ mol^{-1})
First exotherm	146.4	147.2
Second exotherm	111.5	114.6

the plot is the weight change expected from the weight loss of CO_2 on the thermal conversion from polybenzoxazine to polybenzoxazole. In the present study, TGA of poly(*o*PP-an) with the isothermal condition at 400 °C for 1 h under N_2 has also been applied as shown in Fig. 11. A weight loss of 19 wt% is observed after thermal treatment at 400 °C. The measured weight loss is greater than expected for benzoxazole formation alone, indicating that some additional degradation reactions also occurred. The rigidity decreases the mobility of molecules of *o*PP-an during polymerization, which likely results in the low degree of crosslinking, generating terminal defect structures. Thus, the additional weight-loss during benzoxazole formation originates from the degradation of the defect structures of polybenzoxazine networks.

The structural conversion from benzoxazine to polybenzoxazole was further confirmed by solid-state ^{13}C NMR with cross-polarization magic-angle spinning (CP-MAS) as shown in Fig. 12. In accordance with the ^{13}C NMR spectrum of *o*PP-an in solution, the characteristic solid ^{13}C resonances of the oxazine ring are assigned at 54 and 78 ppm for Ar–CH_2–N– and –O–CH_2–N–, respectively. Besides, the characteristic resonance of the nitrile carbon of –C≡N is centered at 105 ppm. Moreover, the spectrum for PBO-*o*PP-an showed drastic differences compared with that of *o*PP-an as expected. The carbon resonances of the oxazine ring and nitrile of *o*PP-an completely disappeared, and a broad signal corresponding to the –CH_2– of the Mannich bridge around 41 ppm as well as a characteristic resonance of triazine at 167 ppm can be observed in the spectrum of PBO-*o*PP-an. These variations suggest the completion of ring-opening polymerization and cyclotrimerization for *o*PP-an after the designed procedure of thermal treatments. In addition, the new carbon resonances at 161, 148 and 142 ppm, which can be assigned to the typical carbon resonances of benzoxazole groups, are well resolved.[42] This difference between the benzoxazine monomer and the final obtained polymer strongly supports the proposed benzoxazole formation from *ortho*-phthalimide-functionalized benzoxazine and is in agreement with other evidence of FTIR and TGA analyses.[19] As a result, the proposed structural transformation mechanism of *o*PP-an can be described as Scheme 2.

Thermal and heat release properties of thermosets

The thermal stability of PBO-*o*PP-an has also been studied by TGA and the result is shown in Fig. 13. The initial decomposition temperatures of 5% and 10% weight losses (T_{d5} and T_{d10}) for PBO-*o*PP-an under an inert atmosphere are as high as 550

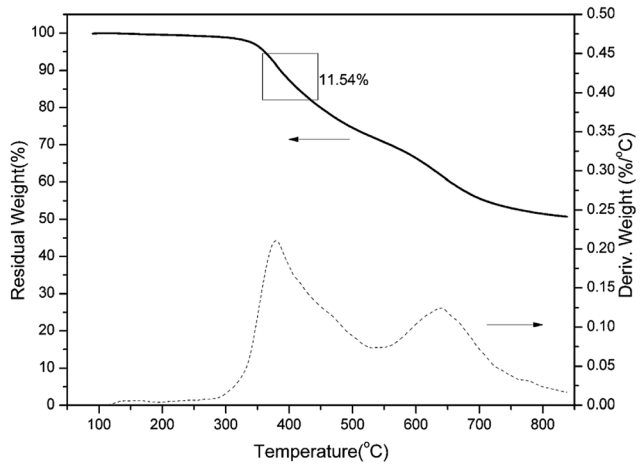

Fig. 10 Thermogravimetric analysis of poly(*o*PP-an). The rectangular box indicates the theoretical weight change upon loss of CO_2 during benzoxazole formation.

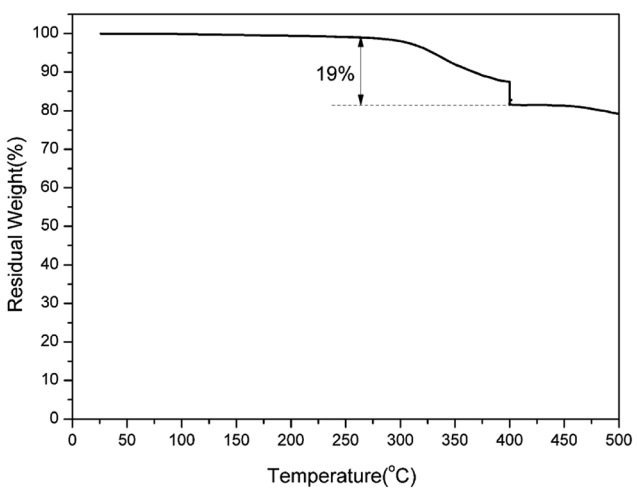

Fig. 11 Thermogravimetric analysis of poly(*o*PP-an). At 400 °C, isothermal heating was applied for 1 h.

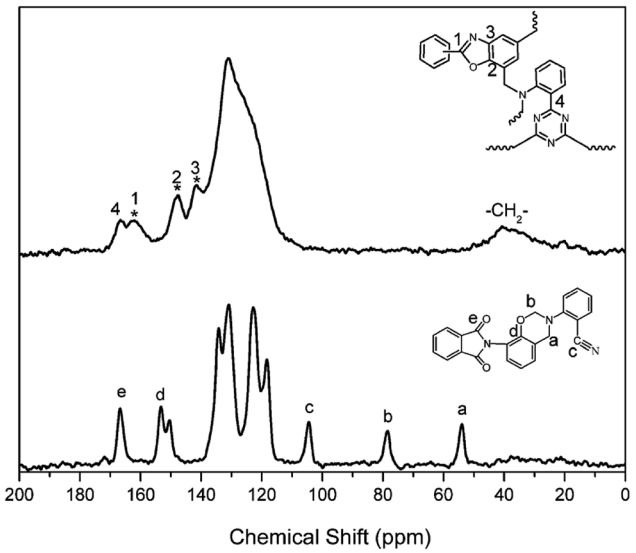

Fig. 12 Solid-state ^{13}C NMR spectra of *o*PP-an and PBO-*o*PP-an.

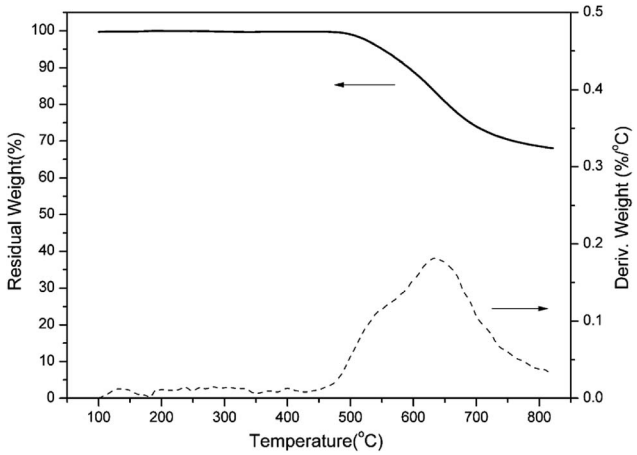

Fig. 13 Thermogravimetric analysis of PBO-*o*PP-an.

and 591 °C, respectively, as a consequence of the oxazole formation. Besides, PBO-*o*PP-an shows a degradation profile in which the maximum weight-loss rate occurs at 637 °C, which is consistent with the degradation temperature of polybenzoxazoles. Furthermore, PBO-*o*PP-an exhibits a very high char yield (Y_c) value of 70% at 800 °C. The thermal property data of PBO-*o*PP-an are summarized in Table 2, which demonstrates the exceptionally high thermal stability of PBO-*o*PP-an.

The LOI parameter of PBO-*o*PP-an can be determined from the Y_c values based on TGA results by using the Van Krevelen equation,[43] from which the LOI value of PBO-*o*PP-an at 800 °C was found to be 45.5. PBO-*o*PP-an has a LOI value in the self-extinguishing region (LOI > 28),[44] suggesting that the cross-linked polybenzoxazole derived from the *ortho*-imide-functionalized benzoxazine containing a nitrile group is a good candidate for applications such as fire resistant and electronic encapsulation materials.

The heat release capacity (HRC) is an effective evaluation parameter of thermal combustion and is one of the best single predictors of the flammability of a material,[45] and was obtained from microscale combustion calorimetry (MCC) in this study. Milligram size samples of poly(*o*PP-an) and PBO-*o*PP-an were tested at a constant heating rate of 1 K s^{-1} over the temperature range 100–900 °C. As shown in Fig. 14, MCC characterization of poly(*o*PP-an) and PBO-*o*PP-an reveals HRC values of 67.3 and 30.1 J g^{-1} K^{-1}, respectively. Besides, poly(-*o*PP-an) exhibits a THR value of 14.8 kJ g^{-1}, while PBO-*o*PP-a shows a much lower THR value of 7.6 kJ g^{-1}. In general, the lower the values of HRC and THR, the higher the flame resistance. The HRC values of both thermosets based on *o*PP-an were much lower than those of the other 47 polymers reported by Lyon *et al.*[45] Furthermore, this new class of thermosets is better than the benzoxazole resins derived from *ortho*-amide benzoxazines, which show HRC values of ~92 J g^{-1} K^{-1}.[42] Thus, introduction of triazine or benzoxazole functionalities into a polybenzoxazine network leads to a substantial HRC reduction. Therefore, this newly developed *ortho*-phthalimide-functionalized benzoxazine monomer containing an *ortho*-nitrile group opens up opportunities for applications that benefit from low flammability resins.

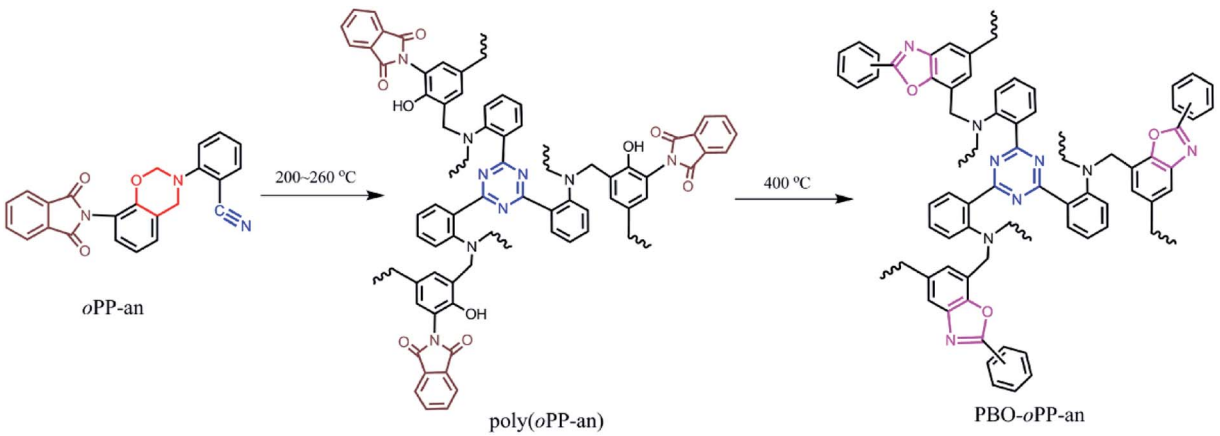

Scheme 2 Polymerization of *o*PP-an generating polybenzoxazine and subsequent thermally induced structural transformation into polybenzoxazole.

Table 2 Thermal and heat release properties of poly(*o*PP-an) and PBO-*o*PP-a

Sample	T_{d5} (°C)	T_{d10} (°C)	Y_c (wt%)	HRC (J g^{-1} K^{-1})	THR (kJ g^{-1})
Poly(*o*PP-an)	362	388	52	67.3	14.8
PBO-*o*PP-an	550	591	70	30.1	7.6

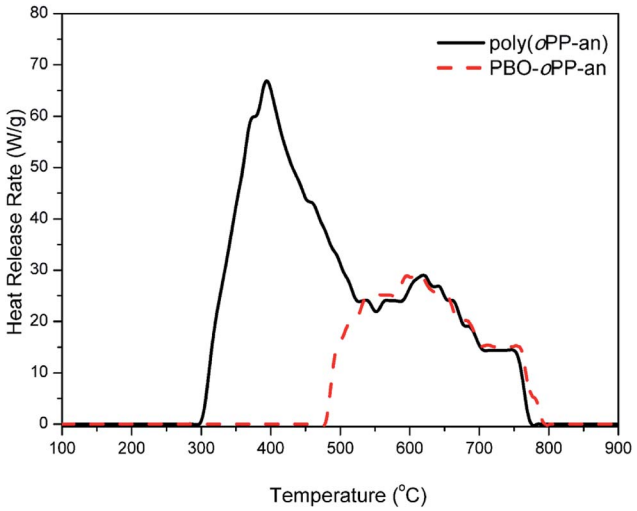

Fig. 14 Heat release rate (HRR) *versus* temperature for poly(*o*PP-an) and PBO-*o*PP-an.

Conclusions

A new *ortho*-phthalimide-functionalized benzoxazine monomer containing an *ortho*-nitrile group has been successfully obtained *via* Mannich condensation. This benzoxazine resin was observed to undergo a special thermally induced structural transformation including ring-opening polymerization, cyclotrimerization and benzoxazole formation. The resulting cross-linked polybenzoxazole derived from the benzoxazine monomer showed exceptionally high thermal stability with a high T_{d5} temperature (550 °C) and high char yield value (70%) and extraordinarily low flammability with a low heat release capacity (HRC of 30.1 J g^{-1} K^{-1}) as well as a very low total heat release (THR of 7.6 kJ g^{-1}). Thus, the combination of the easy synthesis of such a high rigidity compound and the outstanding thermal properties exhibited by thermosets obtained from the same benzoxazine monomer makes *o*PP-an a highly attractive resin for high-performance fields.

Conflicts of interest

There are no conflicts to declare.

Acknowledgements

The authors express their gratitude to the National Natural Science Foundation of China (NSFC) for their financial support (No. 51603093). This project was also supported by the Science and Technology Agency of Jiangsu Province (No. BK20160515), and the China Postdoctoral Science Foundation (No. 2016M600369 and No. 2018T110451).

References

1 G. A. Holmes, K. Rice and C. R. Snyder, *J. Mater. Sci.*, 2006, **41**, 4105–4116.
2 M. H. Dotrong, R. C. Evers and G. Moore, *Polymer Prepr.*, 1990, **31**, 675–676.
3 M. Ueda, H. Sugita and M. Sato, *J. Polym. Sci., Polym. Chem. Ed.*, 1986, **24**, 1019–1026.
4 B. A. Reinhardt, *Polym. Commun.*, 1990, **31**, 453–454.
5 P. J. Walsh, X. Hu, P. Cunniff and A. J. Lesser, *J. Appl. Polym. Sci.*, 2006, **102**, 3517–3525.
6 T. Kubota and R. Nakanishi, *J. Polym. Sci., Part B: Polym. Lett.*, 1964, **2**, 655–659.
7 W. W. Moyer, C. Cole and T. Anyos, *J. Polym. Sci., Part A: Gen. Pap.*, 1965, **3**, 2107–2121.
8 Y. Imai, K. Uno and Y. Iwakura, *Makromol. Chem.*, 1965, **83**, 179–187.
9 M. Ueda, K. Ebara and Y. Shibasaki, *J. Photopolym. Sci. Technol.*, 2003, **16**, 237–242.
10 T. Okabe and A. Morikawa, *High Perform. Polym.*, 2008, **20**, 53–66.
11 H. B. Park, C. H. Jung, Y. M. Lee, A. J. Hill, S. J. Pas, S. T. Mudie, E. V. Wagner, B. D. Freeman and D. J. Cookson, *Science*, 2007, **318**, 254–258.
12 E. Schab-Balcezak, M. Jikei and M. Kamimoto, *Polym. J.*, 2003, **35**, 208–212.
13 D. Guzman-Lucero and D. Likhatcher, *Polym. Bull.*, 2002, **48**, 261–269.
14 B. K. Chen, Y. J. Tsai and S. Y. Tsay, *Polym. Int.*, 2006, **55**, 93–100.
15 S. S. Kim and E. M. Pearce, *Makromol. Chem., Suppl.*, 1989, **15**, 187–218.
16 S. Ohashi, D. Iguchi, T. R. Heyl, P. Froimowicz and H. Ishida, *Polym. Chem.*, 2018, **9**, 4194–4204.
17 H. Ishida, and P. Froimowicz, *Advanced and Emerging Polybenzoxazine Science and Technology*, Elsevier, Amsterdam, 2017.
18 N. N. Ghosh, B. Kiskan and Y. Yagci, *Prog. Polym. Sci.*, 2007, **32**, 1344–1391.
19 K. Zhang, J. Liu, S. Ohashi, X. Liu, Z. Han and H. Ishida, *J. Polym. Sci., Part A: Polym. Chem.*, 2015, **53**, 1330–1338.
20 Z. Deliballi, B. Kiskan and Y. Yagci, *Polym. Chem.*, 2018, **9**, 178–183.
21 K. Zhang and X. Yu, *Macromolecules*, 2018, **51**, 6524–6533.
22 H. Ishida and H. Y. Low, *Macromolecules*, 1997, **30**, 1099–1106.
23 S. B. Shen and H. Ishida, *Polym. Compos.*, 1996, **17**, 710–719.
24 J. Wu, Y. Xi, G. T. McCandless, Y. Xie, R. Menon, Y. Patel, D. J. Yang, S. T. Iacono and R. M. Novak, *Macromolecules*, 2015, **48**, 6087–6095.

25 H. Ishida and D. Allan, *J. Polym. Sci., Part B: Polym. Phys.*, 1996, **34**, 1019–1030.
26 M. W. Wang, C. H. Lin and T. Y. Juang, *Macromolecules*, 2013, **46**, 8853–8863.
27 H. D. Kim and H. Ishida, *J. Phys. Chem. A*, 2002, **106**, 3271–3280.
28 M. W. Wang, C. H. Lin and T. Y. Juang, *Macromolecules*, 2013, **46**, 8853–8863.
29 K. C. Chen, H. T. Li, W. B. Chen, C. H. Liao, K. W. Sun and F. C. Chang, *Polym. Int.*, 2011, **60**, 432–442.
30 A. F. M. El-Mahdy and S. W. Kuo, *Polym. Chem.*, 2018, **9**, 1815–1826.
31 Z. Brunovska and H. Ishida, *J. Appl. Polym. Sci.*, 1999, **73**, 2937–2949.
32 Z. Brunovska, R. Lyon and H. Ishida, *Thermochim. Acta*, 2000, **357**, 195–203.
33 R. E. Lyon and R. N. Walters, *J. Anal. Appl. Pyrolysis*, 2004, **71**, 27–46.
34 K. P. Pramoda, S. L. Liu and T. S. Chung, *Macromol. Mater. Eng.*, 2002, **287**, 931–937.
35 H. Ishida, S. T. Wellinghoff, E. Baer and J. L. Koenig, *Macromolecules*, 1980, **13**, 826–834.
36 B. T. Low, Y. Xiao, T. S. Chung and Y. Liu, *Macromolecules*, 2008, **41**, 1297–1309.
37 T. Agag and T. Takeichi, *Macromolecules*, 2003, **36**, 6010–6017.
38 L. Han, D. Iguchi, P. Gil, T. R. Heyl, V. M. Sedwick, C. R. Arza, S. Ohashi, D. J. Lacks and H. Ishida, *J. Phys. Chem. A*, 2017, **121**, 6269–6282.
39 K. Zhang and H. Ishida, *Polym. Chem.*, 2015, **6**, 2541–2550.
40 H. E. Kissinger, *Anal. Chem.*, 1957, **29**, 1702–1706.
41 T. Ozawa, *J. Therm. Anal.*, 1970, **2**, 301–324.
42 T. Agag, J. Liu, R. Graf, H. W. Spiess and H. Ishida, *Macromolecules*, 2012, **45**, 8991–8997.
43 D. W. Van Krevelen, *Polymer*, 1975, **16**, 615–620.
44 S. Mallakpour and V. Behranvand, *Colloid Polym. Sci.*, 2015, **293**, 333–339.
45 R. E. Lyon and M. L. Janssens, *Polymer Flammability*, U.S. Department of Transportation, Federal Aviation Administration, Report #DOT/FAA/AR-05/14.